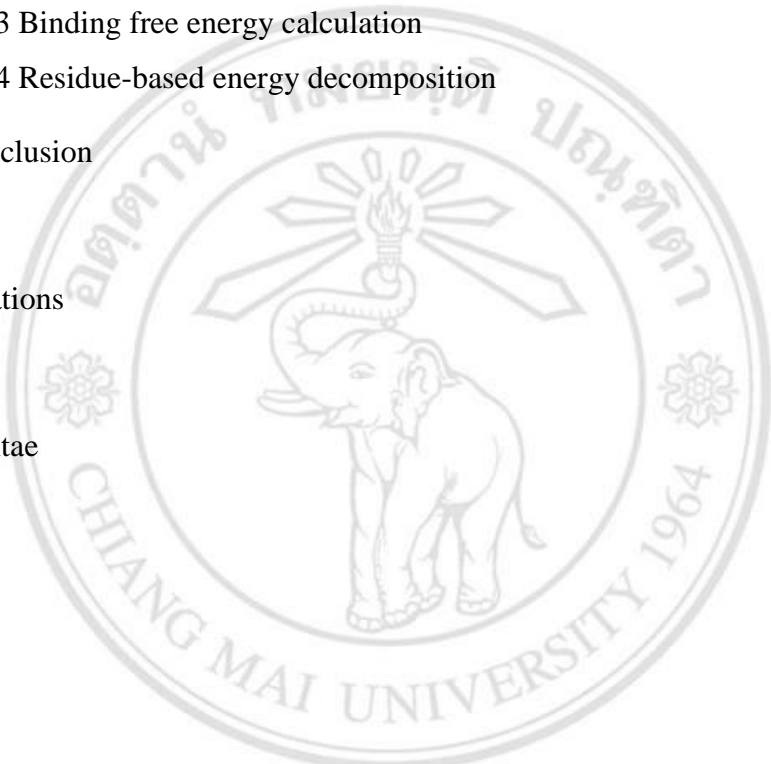


CONTENTS

	Page
Acknowledgement	d
Abstract in Thai	e
Abstract in English	g
List of Tables	l
List of Figures	o
List of Abbreviations	r
List of Symbols	w
Glossary	x
Statement of Originality in Thai	y
Statement of Originality in English	z
Chapter 1 Introduction	1
1.1 Statement and significance of the problem	1
1.2 Literature Review	4
1.3 Hypothesis	79
1.4 Purpose of the study	79
1.5 Research design	79
Chapter 2 Materials and methods	81
2.1 Phytochemical Structures for P-gp inhibitors	81
2.2 QSAR modelling for P-gp inhibitors	81
2.2.1 Preparing of molecular structures	84
2.2.2 Generation of molecular descriptors	85
2.2.3 Statistical methods for QSAR modelling	86

	Page
2.2.4 Validation of a QSAR model	88
2.3 Molecular docking of P-gp inhibitors	89
2.3.1 Preparing of P-gp protein	89
2.3.2 Collection and preparing of ligand molecules	90
2.3.3 Docking method	90
2.3.4 Validation of molecular docking	91
2.3.5 NBD-based pharmacophore identification	92
2.4 Molecular dynamics (MD) simulations of P-gp inhibitors	92
2.4.1 Selection of a model and ligands for MD simulation	92
2.4.2 Preparing of P-gp–ligand complexes for MD simulation	93
2.4.3 MD simulation method	93
2.4.4 Dynamics conformational change analysis of the complexes	94
2.4.5 Pre and post MD simulation binding mode comparison	94
2.4.6 Binding free energy calculation	95
2.4.7 Residue-based energy decomposition	96
Chapter 3 Results and discussion	97
3.1 QSAR analysis	97
3.1.1 QSAR model generation	97
3.1.2 P-gp modulation prediction using the external test set of flavonoids for validation of the generated QSAR model	100
3.2 Molecular docking	105
3.2.1 Docking of P-gp inhibiting compounds against NBD1	105
3.2.2 Correlation between experimental data and NBD1 docking scores	109
3.2.3 NBD1-based pharmacophore modelling (binding mode analysis) for P-gp–ligand interactions	110
3.2.4 Docking of P-gp inhibiting compounds against NBD2	119
3.2.5 Correlation between experimental data and NBD2 docking scores	124

	Page
3.2.6 NBD2-based pharmacophore modelling (binding mode analysis) for P-gp–ligand interactions	125
3.3 Molecular dynamics (MD) simulations of P-gp inhibitors	137
3.3.1 Trajectory analysis	137
3.3.2 Pre and post MD simulation binding mode analysis	139
3.3.3 Binding free energy calculation	149
3.3.4 Residue-based energy decomposition	150
Chapter 4 Conclusion	158
References	160
List of Publications	188
Appendix	189
Curriculum Vitae	195



 ลิขสิทธิ์มหาวิทยาลัยเชียงใหม่
 Copyright© by Chiang Mai University
 All rights reserved

LIST OF TABLES

	Page
Table 1.1 The adverse event number related with herbal products submitted to the Health Product Vigilance Centre, Thai FD	7
Table 1.2 Reports of adverse events caused from various herbal products	8
Table 1.3 Herbal products and dietary supplements used in 56 patients with chronic diseases followed up at Changphuek Health Promoting Hospital	13
Table 1.4 The number of patients with the potential herb/dietary supplement-drug interactions	14
Table 1.5 The number of patients with the potential herb/dietary supplement-drug interactions and possible mechanisms	15
Table 1.6 Some herbs that interact with CYP and efflux proteins	26
Table 1.7 Identified ATP-binding cassette (ABC) transporters	28
Table 1.8 Effect of herbs on transporters	30
Table 1.9 <i>In vivo</i> effects of phytochemicals on pharmacokinetics of some nonmetabolised P-gp substrates	34
Table 1.10 P-gp mediated herb interactions with anticancer drugs	35
Table 1.11 List of P-gp inhibition of pharmacokinetic interactions between Thai herbs and drugs	36
Table 1.12 P-gp and CYP-mediated herb-drug interaction	48
Table 1.13 Substrates of P-glycoprotein (ABCB1)	51
Table 1.14 The instance of classical P-glycoprotein inhibitors by generation	53
Table 1.15 Cellular mechanism of classical inhibitors of P-glycoprotein	53
Table 1.16 List of natural constituents identified as P-gp inhibitors	55
Table 1.17 The theoretic models for prediction of P-gp substrates and inhibitors	57

	Page
Table 1.18 Available crystal structures of ATP-binding cassette transporters along with P-glycoprotein (ABCB1)	66
Table 2.1 Molecular structures of bioflavonoids with FAR values (in the parenthesis) of the training set. 1-21 are from Gyémant et al., and 22-23 are from Martins et al.	83
Table 2.2 Summary of 35 categories comprising 1252 molecular descriptors calculated using ADRIANA.Code	86
Table 2.3 Pharmacophore features from LigandScout	92
Table 3.1 Correlation matrix indicating intercorrelation among descriptors used in MLR QSAR model	98
Table 3.2 The observed and calculated pFAR values using the developed QSAR equation with associated residuals	99
Table 3.3 Comparison between the calculated P-gp modulatory activity values (pFAR) and observed values of 11 flavonoids which exhibited a significant experimental P-gp inhibitory activity expressed by Inhibitory efficiency	101
Table 3.4 The experimental P-gp inhibitory activity value expressed by percentage compared to a positive control (verapamil) and the docking score at NBD1 expressed by the estimated free energy of binding of each flavonoid	106
Table 3.5 Composition of docking energy against NBD1 of each flavonoid	108
Table 3.6 The structure-based pharmacophore models obtained from the docking complex illustrates in the major active cavity of 4Q9H NBD1.	112
Table 3.7 Binding modes of flavonoids, control drugs, and substrate at NBD1	115
Table 3.8 The important amino acid residues of NBD1 that involved in the molecular interactions of P-gp crystal structures (4Q9H) with its inhibitors (flavonoids) identified by LigandScout	119

Table 3.9	The experimental P-gp inhibitory activity value expressed by percentage compared to a positive control (verapamil) and the docking score at NBD2 expressed by the estimated free energy of binding of each flavonoid	121
Table 3.10	Composition of docking energy against NBD2 of each flavonoid	123
Table 3.11	The structure-based pharmacophore models obtained from the docking complex illustrates in the major active cavity of 4Q9H NBD2	127
Table 3.12	Binding modes of flavonoids, control drugs, and substrate at NBD2	130
Table 3.13	The important amino acid residues of NBD2 that involved in the molecular interactions of P-gp crystal structures (4Q9H) with its inhibitors (flavonoids) identified by LigandScout	133
Table 3.14	Contribution of energies to binding free energy of 4Q9H–flavonoid complex	150

LIST OF FIGURES

	Page
Figure 1.1 Mechanisms and outcomes of some enzymes and drug transporters mediated interactions among herbs and conventional drugs	25
Figure 1.2 Schematic illustration of the intestinal epithelium and pathways of drug transport across it in both directions. C illustrates efflux of compounds reverting into the intestinal lumen thus restricting absorption of drug into the blood	32
Figure 1.3 Drawing of the major locations of P-glycoprotein in the body	41
Figure 1.4 P-gp molecular structure model (TM: transmembrane domain)	44
Figure 1.5 Flippase model. P-gp reciprocates substrate molecules from the cell membrane's inner leaflet to the outer leaflet, so that it keeps a concentration balance of the substrate on both sides	47
Figure 1.6 Hydrophobic vacuum cleaner mechanism. (I) Substrate molecule penetrate the cell membrane to the lipid bilayer; (II) the substrate molecule can get in the P-gp via portals that impart its substrate from the lipid bilayer into the internal cavity of P-gp; (III) the substrate molecule bind to their binding site; (IV) P-gp transposes the substrate molecule to the extracellular space	47
Figure 1.7 The showing the synergistic role of CYP3A enzymes and the efflux transporter P-glycoprotein (P-gp). After being uptaken by enterocytes, some of the drug molecules are metabolised by CYP3A4. Drug molecules which get away metabolic conversion are disposed from the cells into the lumen via P-gp	49
Figure 1.8 Schematic representation of the calcein AM extrusion assay	78
Figure 1.9 An overview of the research	80

- Figure 3.1 A plot of observed (experimental) versus calculated (predicted) pFAR values of the training set 99
- Figure 3.2 The binding patterns of the flavonoids on NBD1 of P-gp (white) visualised by PyMol. The binding cavity occupied by the most flavonoids (green), controls (magenta), and ATP (orange) is shown as a close-up inside NBD1 as the major binding site except 6a,12a-dehydroamorphigenin and 5HHMF (blue) bind NBD1 at their own distinct cavities 109
- Figure 3.3 Correlation between docking scores (estimated free energies of binding) of flavonoids at NBD1 and percentage of inhibitory efficiency values 110
- Figure 3.4 The binding patterns of the inhibitors on NBD2 of P-gp (white). The binding cavity occupied by the most flavonoids (green), controls (magenta) and ATP (orange) is shown as a close-up inside NBD2 as the major binding site. Formononetin, chrysin, catechin, naringin, and naringenin (blue) bind NBD2 at another pocket as the minor binding site 124
- Figure 3.5 Correlation between docking scores (estimated free energies of binding) of flavonoids at NBD2 and percentage of inhibitory efficiency values 125
- Figure 3.6 Plot of root mean square deviations (RMSD) versus time (ps) obtained over a time course of 15000 ps production for (a) the backbone atom (C_{α} , N, C) of the protein–ligand complexes, (b) NBD2-Cytosolic residues, and (c) ligands 139
- Figure 3.7 Structure-based pharmacophore models illustrate molecular interactions of 4Q9H–amorphigenin. (a) pre-MD interactions, (b) post-MD interactions of the average structure throughout the stable stage (10000-15000 ps), and (c) new formed hydrogen bond distances between 4Q9H–amorphigenin throughout the stable stage 141

- Figure 3.8 Structure-based pharmacophore models illustrate molecular interactions of 4Q9H–chrysin. (a) pre-MD interactions, (b) post-MD interactions of the average structure throughout the stable stage (10000-15000 ps), and (c) a new formed hydrogen bond distance between 4Q9H–chrysin throughout the stable stage 143
- Figure 3.9 Structure-based pharmacophore models illustrate molecular interactions of 4Q9H–epigallocatechin. (a) pre-MD interactions, (b) post-MD interactions of the average structure throughout the stable stage (10000-15000 ps), and (c) new formed hydrogen bond distances between 4Q9H– epigallocatechin throughout the stable stage 145
- Figure 3.10 Structure-based pharmacophore models illustrate molecular interactions of 4Q9H–formononetin. (a) pre-MD interactions, (b) post-MD interactions of the average structure throughout the stable stage (10000-15000 ps), and (c) a new formed hydrogen bond distance between 4Q9H–formononetin throughout the stable stage 147
- Figure 3.11 Structure-based pharmacophore models illustrate molecular interactions of 4Q9H–rotenone. (a) pre-MD interactions, (b) post-MD interactions of the average structure throughout the stable stage (10000-15000 ps), no hydrogen bonds is formed throughout the stable stage 148
- Figure 3.12 Structure-based pharmacophore models illustrate molecular interactions of 4Q9H–verapamil. (a) pre-MD interactions, (b) post-MD interactions of the average structure throughout the stable stage (10000-15000 ps), no hydrogen bonds is formed throughout the stable stage 149
- Figure 3.13 Relative decomposed free energies during 15000 ps of important amino acid residues of 4Q9H NBD2 interacting with all flavonoids and verapamil 151

LIST OF ABBREVIATIONS

ABC	ATP-Binding Cassette
ABCB1	ATP-Binding Cassette Subfamily B Member 1
ABCB11	ATP-Binding Cassette Subfamily B Member 11
ABCC2	ATP-Binding Cassette Subfamily C Member 2
ABCG2	ATP-Binding Cassette Subfamily G Member 2
ADP	Adenosine Diphosphate
AP	Atom Pair
Ar	Aromatic Ring
atm	Standard Atmosphere
ATP	Adenosine Triphosphate
AUC	Area Under The Curve
$AUC_{\text{bile}}/AUC_{\text{blood}}$	Blood-to-Bile Distribution Ratio
BBB	Blood-Brain Barrier
BCRP	Breast Cancer Resistance Protein
bps	Base Pairs
BRNN	Bayesian-Regularised Neural Network
BSEP	Bile Salt Exporting Pump
Caco-2	Human Colonic Adenocarcinoma
CAM	Complementary and Alternative Medicine
CHARMM	Chemistry at Harvard Macromolecular Mechanics
C_{max}	Maximum (or Peak) Serum Concentration
CNS	Central Nervous System
COL	Colchicine
CoMFA	Comparative Molecular Field Analysis
CoMSIA	Comparative Molecular Similarity Index Analysis
CPPIs	Cyclic Peptide Inhibitors
CYP450	Cytochromes P450
DAG	Diacylglycerol

DDI	Drug-Drug Interaction
desolv	Desolvation
DOPC	Dioleoyl-Phosphatidylcholine
DT	Decision Tree
ECG	Epicatechingallate
EC ₅₀	Half Maximal Effective Concentration
EGCG	Epigallocatechingallate
ELE	Non-Bonded Electrostatic Energy
F	Fisher Test
FAR	Fluorescence Activity ratio
FDA	Food and Drug Administration
FFD	Fractional Factorial Design
FLAP	Fingerprints for Ligands and Proteins
GA	Glycyrrhetic Acid
GB	Polar Contribution of Solvation
GB _{SUR}	Non-Polar Contribution to Solvation
GB _{TOT}	Total Binding Free Energy Calculated by the MM-GBSA Method
GI tract	Gastrointestinal Tract
GP	General Practitioner
GPU	Graphics Processing Unit
GSH	Glutathione
HBA	Hydrogen Bond Acceptor
HBD	Hydrogen Bond Donor
HisP	Histidine Permease
HIV	Human Immunodeficiency Virus
HM	Heuristic Method
HVC	Hydrophobic Vacuum Cleaner
IC ₅₀	Half Maximal Inhibitory Concentration
INT	Internal Energies (Bond, Angle, dihedral energies)
K	Kelvin
k _a	Absorption Rate Constants

kcal/mol	Kilocalorie per Mole
K_d	Dissociation Constant
K_i	Inhibitory Constant
k_{NN}	k -Nearest Neighbors
LDA	Linear Discriminant Analysis
LLC-PK1	Porcine Kidney Epithelial
LOO	Leave-One-Out
LTO	Leave-Two-Out
MD	Molecular Dynamics
MDCK	Madin-Darby Canine Kidney
MDR	Multiple Drug Resistance
MDRR	Multiple Drug Resistance Reversal
MLR	Multiple Linear Regression
MM-GBSA	Molecular Mechanic-Generalised Born Surface Area
MM-PBSA	Molecular Mechanics-Poisson-Boltzmann Surface Area
MM2	Molecular Mechanics
MOE	Molecular Operating Environment
mRNA	Messenger Ribonucleic Acid
MRP2	Multidrug Resistance-Associated Protein-2
NBD	Nucleotide Binding Domain
nm	Nanometer
NMR	Nuclear Magnetic Resonance
NPT	Isothermal-Isobaric Ensemble
ns	Nanosecond
NVT	Canonical Ensemble
OATP	Organic Anion-Transporting Polypeptide
PB _{CAL}	Polar Contribution of Solvation
PBMC	Peripheral Blood Mononuclear Cell
PB _{SUR}	Non-Polar Contribution to Solvation
PB _{TOT}	Total Binding Free Energy Calculated by the MM-PBSA Method
PDB	Protein Database

P-gp	P-Glycoprotein
Pi	Inorganic Phosphate
PLS	Partial Least-Squares
PLSD	Partial Least Square Discriminant Analysis
PME	Particle Mesh Ewald
PMEMD	Particle Mesh Ewald Molecular Dynamics
PMF	Polymethoxyflavone
ps	Picoseconds
q^2	Cross-Validated R^2
QSAR	Quantitative Structure-Activity Relationship
RDF	Radial Distribution Functions
RF	Reversal Factor
RG	Random Grouping
RMS	Root-Mean-Square
RMSD	Root Mean Square Deviations
RMSE	Root-Mean-Square Error
RP	Recursive Partitioning
r	Pearson's Correlation Coefficient
R^2	Coefficient of Determination
R^2_{adj}	Adjusted Coefficient of Determination
R^2_{Pred}	R-Squared Predicted
SAR	Structure-Activity Relationship
SEE	Standard Error of Estimate
SLC	Solute Linked Carrier
SMILES	Simplified Molecule Input Line Entry System
SOM	Self-Organising Map
SVM	Support Vector Machine
$T_{1/2}$	Apparent Terminal Elimination Half-Life Time
TCAs	Tricyclic Antidepressants
TCM	Traditional Chinese Medicines
TM	Transmembrane
T_{max}	Time Taken to Reach the Maximum Concentration

TMD	Transmembrane Domains
UGT	UDP-Glucuronosyltransferase
UV	Use Values
vdW	Van Der Waals Forces
VMD	Visual Molecular Dynamics
3D-QSAR	Three Dimensional Structure-Activity Relationships
^3H	Tritium
5HHMF	5-Hydroxy-3,6,7,8,3',4'-Hexamethoxyflavone
^{125}I	Iothalamate



ลิขสิทธิ์มหาวิทยาลัยเชียงใหม่
 Copyright© by Chiang Mai University
 All rights reserved

LIST OF SYMBOLS

Å	angstrom
+	plus
-	minus
±	plus-minus
=	equality
>	greater than
<	less than
%	percent
Σ	summation
α	alpha
β	beta
Δ	delta
μ	micro
σ	sigma
π	pi
C _α	alpha carbon
ΔG _{binding}	the change in binding free energy
μM	micromolar

ลิขสิทธิ์มหาวิทยาลัยเชียงใหม่
Copyright© by Chiang Mai University
All rights reserved

GLOSSARY

- AMBER** "Amber" refers to two things: a set of molecular mechanical force fields for the simulation of biomolecules (which are in the public domain, and are used in a variety of simulation programmes); and a package of molecular simulation programmes.
- AUTODOCK** AutoDock is a suite of automated docking tools. It is designed to predict how small molecules, such as substrates or drug candidates, bind to a receptor of known 3D structure.
- LIGANDSCOUT** LigandScout is computer software that allows creating three-dimensional (3D) pharmacophore models from structural data of macromolecule–ligand complexes, or from training and test sets of organic molecules. It incorporates a complete definition of 3D chemical features (such as hydrogen bond donors, acceptors, lipophilic areas, positively and negatively ionisable chemical groups) that describe the interaction of a bound small organic molecule (ligand) and the surrounding binding site of the macromolecule.
- SPSS** SPSS Statistics is a software package used for statistical analysis. Long produced by SPSS Inc., it was acquired by IBM in 2009. The current versions (2015) are officially named IBM SPSS Statistics. Companion products in the same family are used for survey authoring and deployment (IBM SPSS Data Collection), data mining (IBM SPSS Modeler), text analytics, and collaboration and deployment (batch and automated scoring services).

ข้อความแห่งการริเริ่ม

- 1) เนื้อหาของวิทยานิพนธ์ฉบับนี้เป็นผลจากการวิจัยที่เป็นต้นฉบับของทางผู้วิจัยเอง ซึ่งได้ดำเนินการภายใต้การกำกับดูแลของอาจารย์ ดร. สุวัฒน์ จิรานุสรณ์กุล
- 2) ใช้วิธีการทำนายฤทธิ์การปรับเปลี่ยนการทำงานของพี-จีพี โดยการพัฒนา QSAR อย่างง่ายซึ่งสามารถนำไปใช้และให้ประสิทธิภาพสูงในการทำนายฤทธิ์ดังกล่าว
- 3) การประยุกต์ใช้วิธี โมเลกุลดาร์ต็อกกิ่ง โดยใช้สารไบโอฟลาโวนอยด์ 25 ตัวเข้าจับกับตำแหน่งเกาะของนิวคลีโอไทด์ของพี-จีพี เพื่อสร้างสารประกอบเชิงซ้อนของโปรตีน-ลิแกนด์ เพื่อหาปัจจัยทางเคมีกายภาพซึ่งมีความเกี่ยวข้องกับการยับยั้งพี-จีพีของฟลาโวนอยด์ส่วนมากโดยผ่านกลไกการยับยั้งแบบแข่งขันการเข้าจับในตำแหน่งดังกล่าวกับเอทีพี
- 4) วิธีการจำลอง โมเลกุลพลวัตสำหรับการวิเคราะห์ปฏิกิริยาในระดับโมเลกุลระหว่างฟลาโวนอยด์ (ที่มีฤทธิ์ยับยั้งการทำงานของพี-จีพีที่สูง) กับ NBD2 ช่วยให้ทราบถึงข้อมูลเชิงลึกของกลไกการยับยั้งดังกล่าวของสารเหล่านี้

ลิขสิทธิ์มหาวิทยาลัยเชียงใหม่
Copyright© by Chiang Mai University
All rights reserved

STATEMENTS OF ORIGINALITY

1. The contents of this thesis are the result of my original research, which has been conducted under the principal supervision of Dr. Supat Jiranusornkul.
2. The predicting method of P-gp modulatory activity using developed facile QSAR model is applied and gives a high predicting efficacy.
3. The molecular docking method used to dock 25 bioflavonoids to P-gp nucleotide binding domains (NBDs) is applied to generate protein-ligand complexes that are used to clarify physiochemical factors relating with the most flavonoids that are essential for P-gp inhibition by an ATP competitive mechanism at NBDs.
4. The molecular dynamics (MD) simulation method for analysis of molecular interactions between flavonoids (which exhibit P-gp strong inhibitory activities) and NBD2 provided a deeper and better insight into the mechanisms of inhibition of these compounds.

ลิขสิทธิ์มหาวิทยาลัยเชียงใหม่
Copyright© by Chiang Mai University
All rights reserved